PAPER

Mechanically metastable structures generated by single pulse laser-induced periodic surface structures (LIPSS) in the photoresist SU8

To cite this article: Hendrik Reinhardt *et al* 2018 *Nanotechnology* **29** 305303

IOP Publishing Nanotechnology
Nanotechnology **29** (2018) 305303 (7pp) https://doi.org/10.1088/1361-6528/aac378

Mechanically metastable structures generated by single pulse laser-induced periodic surface structures (LIPSS) in the photoresist SU8

Hendrik Reinhardt, Patrick Peschke, René Riedel and Norbert Hampp

Department of Chemistry, Philipps-University of Marburg, D-35032 Marburg, Germany

E-mail: Hendrik.Reinhardt@staff.uni-marburg.de

Received 15 February 2018, revised 17 April 2018
Accepted for publication 9 May 2018
Published 22 May 2018

Abstract

Laser-induced periodic surface structures (LIPSS) with a periodicity of 351 nm are generated in the negative photoresist SU8 by single nanosecond laser pulse impact. Friction scans indicate the periodic pattern to comprise alternating regions of crosslinked and non-crosslinked SU8. Intriguingly, even minor mechanical stimuli in the order of nanonewtons cause the unfolding or rather the deletion of the characteristic periodic pattern similarly to the release of a pre-loaded spring. This feature combined with high resilience to heat and photon irradiation makes SU8-LIPSS attractive for applications such as mechanical stress monitors, self-destructing memory and passive micro actuators.

Keywords: laser-induced periodic surface structures, LIPSS, photoresist SU8, mechanically metastable surface

(Some figures may appear in colour only in the online journal)

Introduction

In search for functional surfaces, nature has always been a paragon of smart designs to learn from [1]. Like for the gecko feet, these functionalities are often based on nanoscopic surface structures [2]. Over the years, material scientists developed a wide portfolio of techniques for pattern formation on surfaces [3–7]. Lithographic methods such as electron beam- or nanoimprint lithography are frequently applied for the generation of micro- and nanostructures although they are rather cost-intensive and inflexible in operation [8–10]. Laser-based techniques represent an attractive alternative as they are comparatively cost-efficient and enable the formation of various pattern types. Besides their classical application as a tool for macro- and microstructure formation, lasers also provide the opportunity to generate nanostructures in a fast and efficient way through the exploitation of self-organization processes [11–13]. In particular, a phenomenon called laser-induced periodic surface structures (LIPSS) offers great potential for the implementation of self-organization into technical fabrication. Discovered by M Birnbaum in the mid 1960s, LIPSS are still under intensive research as they are intriguing for practical applications as well as fundamental research since their mechanism of formation is still not fully understood [14–16]. Even though several theories have been proposed, a common perception sees LIPSS originating from the interference of an incident laser wavefront with surface plasmon polaritons [17–21]. Inhomogeneous energy absorption is expected as the major driving force that transforms affected surfaces into the typically observed structure of periodic ripples whose periodicity and orientation depend on parameters such as the laser wavelength, angle of incidence and polarization as well as on the properties of the irradiated material [22]. There are numerous examples of LIPSS formation on inorganic materials such as metals, semiconductors and dielectrics. Moreover, LIPSS can be generated on frequently used polymers such as polyethylene terephthalate, polystyrene, poly(trimethylene terephthalate) and polycarbonate bisphenol A, as well as on the naturally-derived polymer chitosan and on the conjugated polymer poly(3-hexylthiophene), to name a few

[23–25]. In this work we present the formation of LIPSS on SU8, a prominent photoresist frequently used in MEMS fabrication [26–28]. In contrast to above mentioned polymers, SU8 is a negative photoresist that undergoes crosslinking upon exposure to UVA irradiation. Crosslinking is triggered by photochemical acid generation which leads to inter- and intramolecular reactions of epoxy groups. In 2016, He *et al* demonstrated sub-diffraction limited writing in SU8 by exploiting LIPSS as a tool to improve the lateral resolution of a femtosecond laser system well below 100 nm [29]. Their results confirm that SU8 is well suited for the recording of pulsed laser-induced events. In the present study, this property is utilized for investigations on LIPSS formation on SU8 by nanosecond pulsed lasers. We found that LIPSS formation on SU8 is triggered by a single nanosecond laser pulse at a wavelength of 355 nm. Commonly, LIPSS are formed as a result of multiple overlapping laser pulses. The formation of LIPSS resulting from a single laser pulse impact is rarely observed, though not unknown [30]. Atomic force microscopy (AFM) on as-generated SU8-LIPSS indicates that the periodic structure comprises alternating regions of crosslinked and non-crosslinked photoresist. AFM analyses also reveal that SU8-LIPSS feature a rather special mechanically behavior: touching SU8-LIPSS with an AFM-tip repeatedly leads to the disappearance of the periodic pattern. Considering that an AFM-tip exerts forces in the order of nanonewtons to the substrate, this demonstrates SU8-LIPSS to be very sensitive to mechanical stimulation. Surprisingly, the periodic pattern is compromised neither by exposure to heat nor photon irradiation but immediately erased by electron irradiation and mechanical stimulation.

Methods

Coating of SU8 thin films on silicon wafers

SU8 thin films were coated on silicon wafers by spin coating. SU8-100 (MicroChem, Newton, MA 02464, USA) was diluted with γ-butyrolactone (GBL) (50% w/w). Silicon wafers thickness 650 μm, orientation $\langle 100 \rangle$, resistivity 2.1 $\Omega\,cm^{-1}$, and surface finish SPP (Siegert Wafer, Product-No. W16021, Germany) were diced into pieces and cleaned thoroughly with a solution of KOH (1 $mol\,l^{-1}$) and Isopropanol (1:1). Spin coating was performed on a Spin150 coater (ATP, Germany). In a typical run, 0.3 ml of diluted SU8-100 was deposited in the center of a wafer substrate and spread out over the surface by spinning at 500 rpm for 5 s followed by spinning at 2000 rpm for 40 s. Subsequently, SU8 was soft-baked for 3 min at 95 °C in accordance to the official SU8 manual. Typical film thicknesses obtained by this procedure are in the range of 1 μm.

Laser irradiation of SU8 thin films on silicon

Experiments were conducted using two different nanosecond pulsed laser systems that differ primarily in terms of the pulse repetition rate. Both systems emit a wavelength of 355 nm (UVA) generated via frequency tripled Nd:YAG or Nd:YVO_4, respectively.

The diode-pumped solid state laser AViA 355-7000 (Coherent, USA) operates in spatial mode TEM_{00} (Gaussian intensity profile) and emits laser pulses of appr. 20 ns pulse length in a pulse repetition range of 10–100 kHz. The laser beam is steered over specimens via a galvanometer scan head (SS-III-15, Raylase, Germany) equipped with a telecentric F-Theta lens (S4LFT4262/075, Sill Optics, Germany) which focuses the laser beam to a spot size of 20 μm diameter (1 e^{-2}).

The flash light-pumped solid state laser QuickLaze 50STII Trilite (New Wave Research, USA) operates at a pulse repetition rate of 1 Hz and a pulse length of 3 ns. The spatial intensity distribution of the laser beam is top hat and can be further modified by an aperture stop. Using an internal aperture value of 40 × 40, the laser spot on the specimen was determined to be about 700 μm^2 when the beam was focused through an objective lens with 50× magnification (M Plan Apo NUV, Mitutoyo, Japan). Samples are scanned by a precision xy-translation stage.

For both systems, the laser power incident to substrates was measured with a FieldMaxII power meter (Coherent, USA).

Inspection of samples

Topography scans were performed on a laser scanning microscope (LSM 5 Pascal, Carl Zeiss, Germany). AFM was conducted on a Nanoscope IV (Bruker, USA) equipped with a Multimode 8 scanner and SNL-10 tips. Scanning electron microscopy was performed on a JSM7500F (Jeol, Japan) or rather a VEGA3 (TESCAN, Czech Republic) which served as the electron source for LIPSS-deletion experiments.

Results and discussion

LIPSS formation demands specific irradiation conditions which largely depend on the properties of the material to be modified. In order to identify suitable irradiation conditions, systematic screening of various irradiation parameters is required. For the system under investigation here (silicon supported SU8 thin films), screenings were initially performed with the diode-pumped solid state laser system Coherent AViA (355 nm). Despite a large number of conditions arranged by varying laser parameters such as pulse energy, pulse repetition rate, scan speed or rather laser fluence, no set of parameters led to the formation of LIPSS on SU8. A typical result is exemplified in figure 1. The surface of SU8 is unaffected by irradiation with a laser fluence of 0.08 $J\,cm^{-2}$. Developing groves observed on samples subjected to 0.28 $J\,cm^{-2}$ feature remote similarities to commencing LIPSS formation, however, these first signs of pattern formation disappear with increasing energy input. Excessive heat accumulation caused by laser stimulation of the polymer thin film with high rates of pulse repetition may be the reason for this behavior. From the studies of Rodriguez, Barb, and

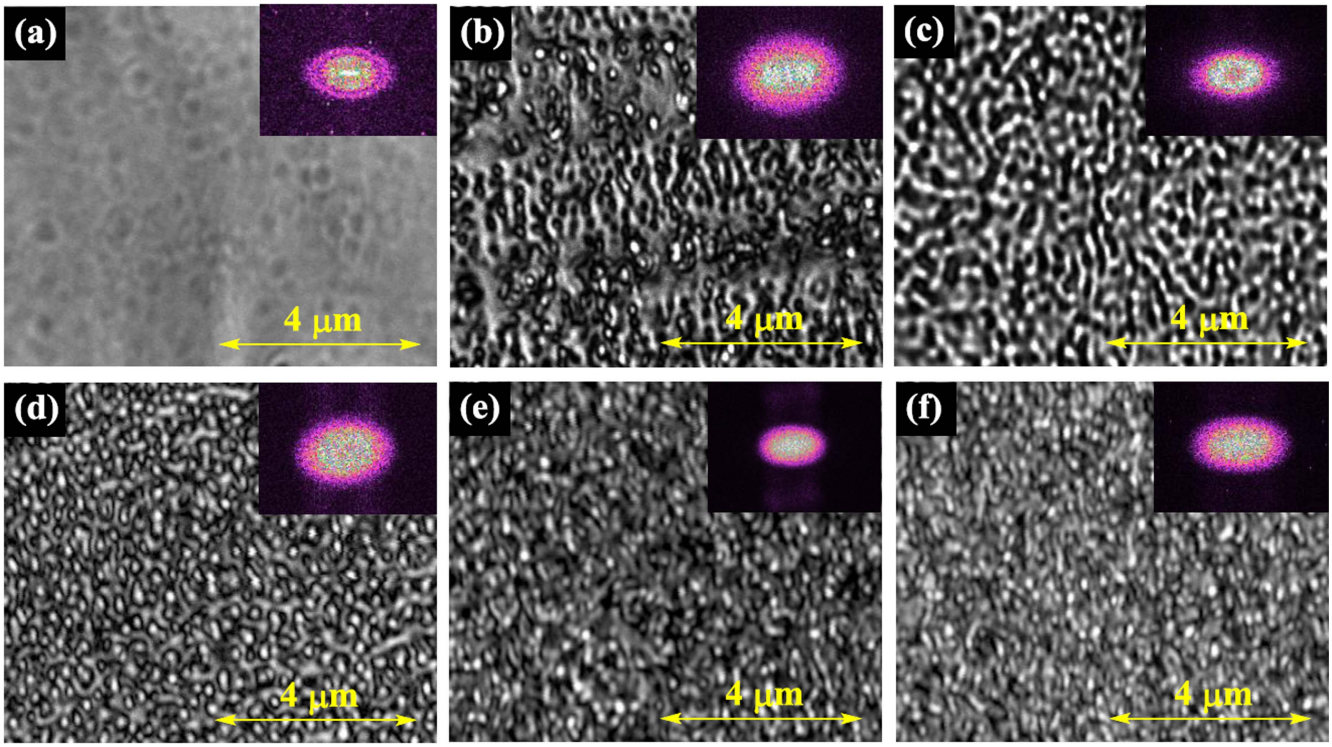

Figure 1. Laser scanning microscope (LSM)-images of SU8 thin film on silicon after irradiation with increasing laser fluences at 50 kHz pulse repetition rate. Fast Fourier transformations (FFT) are given in the top right corners. (a) 0.08 J cm^{-2}, (b) 0.28 J cm^{-2}, (c) 1.15 J cm^{-2}, (d) 2.4 J cm^{-2}, (e) 6.1 J cm^{-2}, (f) 9.14 J cm^{-2}.

Rebollar, it can be concluded that LIPSS formation on polymers is usually achieved with low frequency lasers (repetition rates < 100 Hz) [23–25]. Hence, experiments were continued with the QuickLaze 50STII Trilite emitting 3 ns pulses at 355 nm wavelength and a pulse frequency of 1 Hz. Results are presented in figure 2. A single pulse with a fluence of 0.05 J cm^{-2} does not cause any morphological changes to the SU8 thin film. When the laser fluence is raised to 0.1 J cm^{-2} the damage threshold of the SU8 film is evidently surpassed. Further increases of laser fluence initially result in extended damage of the SU8 film. At 0.18 J cm^{-2}, however, irradiation conditions for LIPSS formation on SU8 are spontaneously met. The periodicity of the resulting SU8-LIPSS was determined to be 351 nm which is close to the theoretically expected periodicity derived from Emmony's surface scattered wave theory for LIPSS generation by a nanosecond laser of 355 nm wavelength at 90° angle of incidence [15]. The mechanism of LIPSS formation is based on interference between incident laser wave fronts and reflected waves which leads to inhomogeneous energy input into the surface resulting in periodic modification [31]. LIPSS in SU8 are oriented parallel with regard to the laser polarization. Remarkably, the laser fluence of 0.18 J cm^{-2} lies exactly in between the fluences used in the experiments with the high frequency laser (figures 1(a), (b)) which either left the surface of SU8 unaffected or started to reconstruct its morphology into a ripple-like but rather disordered structure. This shows that the pulse rate is a major determining factor for LIPSS formation on SU8. In order to obtain a deeper understanding of LIPSS on SU8, the surface was inspected with AFM. Scans were performed at a scan angle of 90° with respect to the orientation of the SU8-LIPSS. The results confirm that periodic structures observed with laser-scanning microscopy (LSM) are indeed morphological features on the surface of the photopolymer (figure 3(a)). Accordingly, LIPSS generated with a single pulse of 0.18 J cm^{-2} have a peak-to-valley height of approximately 30 nm (figures 3(b), (c)). Parallel to the topography scans the friction of the AFM tip on SU8-LIPSS was recorded (figure 3(d)). SU8-LIPSS display in the friction scan, however, peaks in the friction scan are located in the topographical valleys of SU8-LIPSS (compare figures 3(b) and (e)). Nanotribology is strongly affected by the chemical nature of a material, thus indicating friction scans to display alternating regions of crosslinked and non-crosslinked SU8. Friction scans across the border from irradiated to non-irradiated sections of SU8 confirm this assumption (figure 3(f)). The finding that SU8-LIPSS contains alternating regions of crosslinked and non-crosslinked epoxy resin is intriguing as it indicates LIPSS to originate from well defined photonic fringe patterns that build up on the surface of solids under specific conditions of pulsed laser irradiation. In the course of friction measurements on SU8-LIPSS yet another interesting phenomenon was discovered: the acquisition of AFM scans turned out to be challenging due to the complicated surface morphology of SU8-LIPSS. As the LSM scan in figure 2(e) suggests, SU8-LIPSS are not planar but rather curved and partly detached from the wafer substrate. Especially the latter turned out to be problematic as AFM tips tend to collide or stick to SU8-LIPSS. Albeit complicating AFM scans, mentioned problems led to the

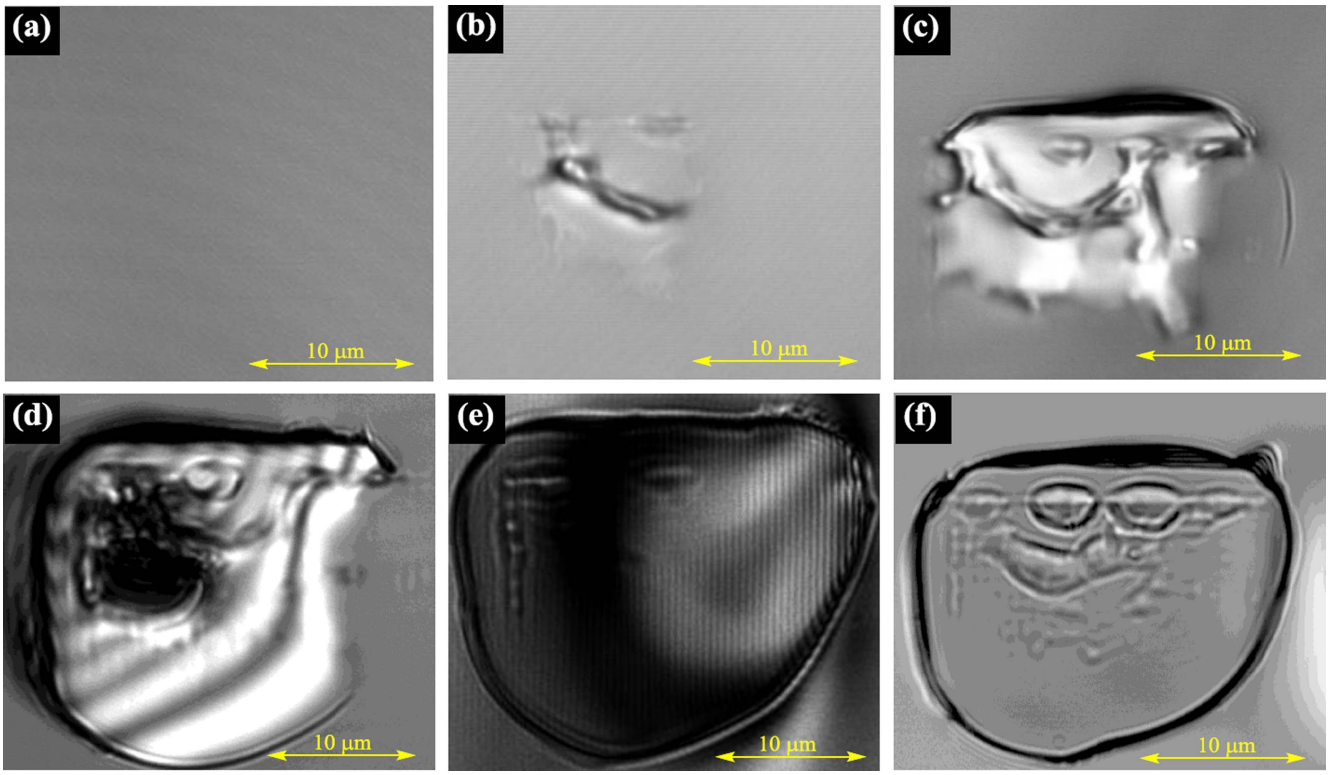

Figure 2. LSM-images of SU8 thin films on silicon each modified with a single 3 ns pulse at varying fluences: (a) 0.05 J cm^{-2}, (b) 0.1 J cm^{-2}, (c) 0.15 J cm^{-2}, (d) 0.17 J cm^{-2}, (e) 0.18 J cm^{-2}, (f) 0.2 J cm^{-2}. The film thickness of SU8 is 0.93 μm.

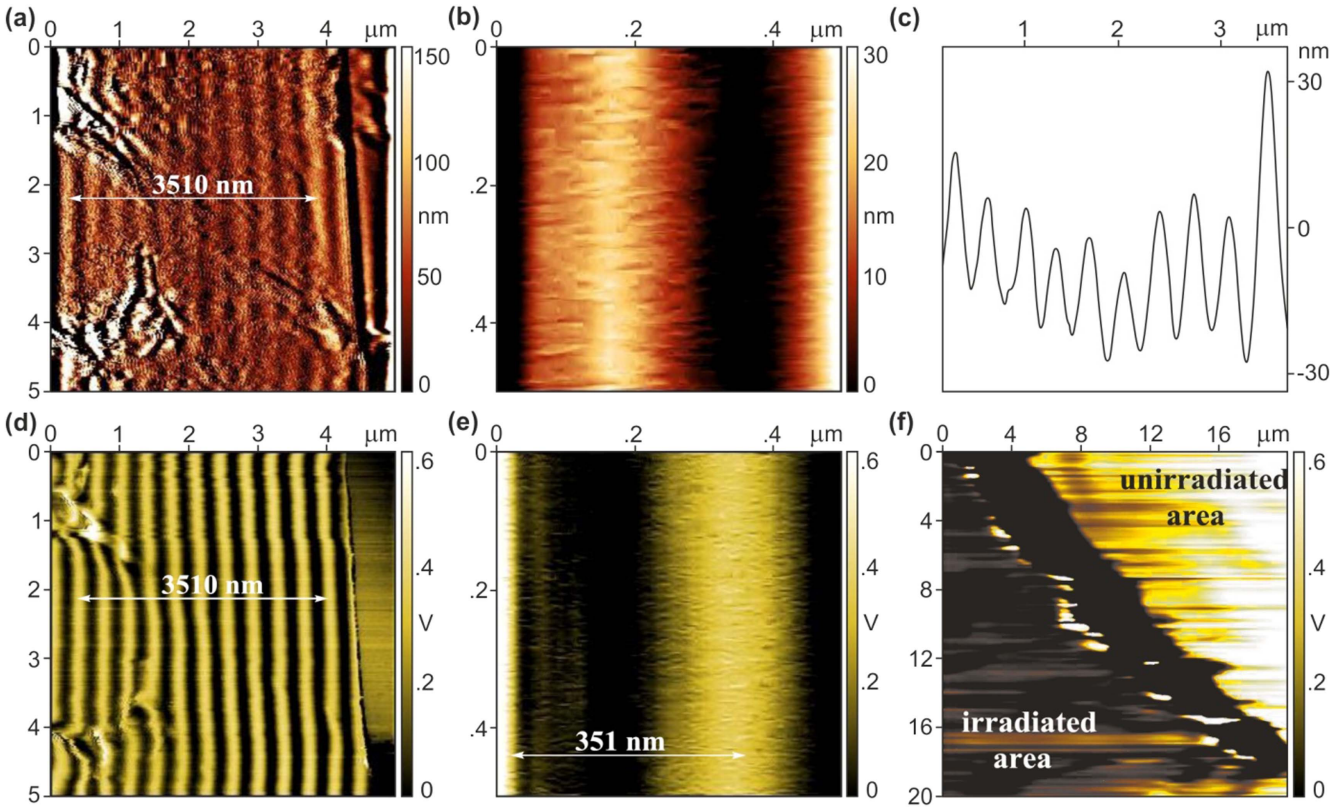

Figure 3. AFM-scans of SU8-laser-induced periodic surface structures (LIPSS) generated by a single pulse at a fluence of 0.18 J cm^{-2} (a), (b) topography scans of SU8-LIPSS, (c) cross section of SU8-LIPSS topography, (d), (e) friction scans of SU8-LIPSS, (f) friction scan of irradiated and unirradiated SU8.

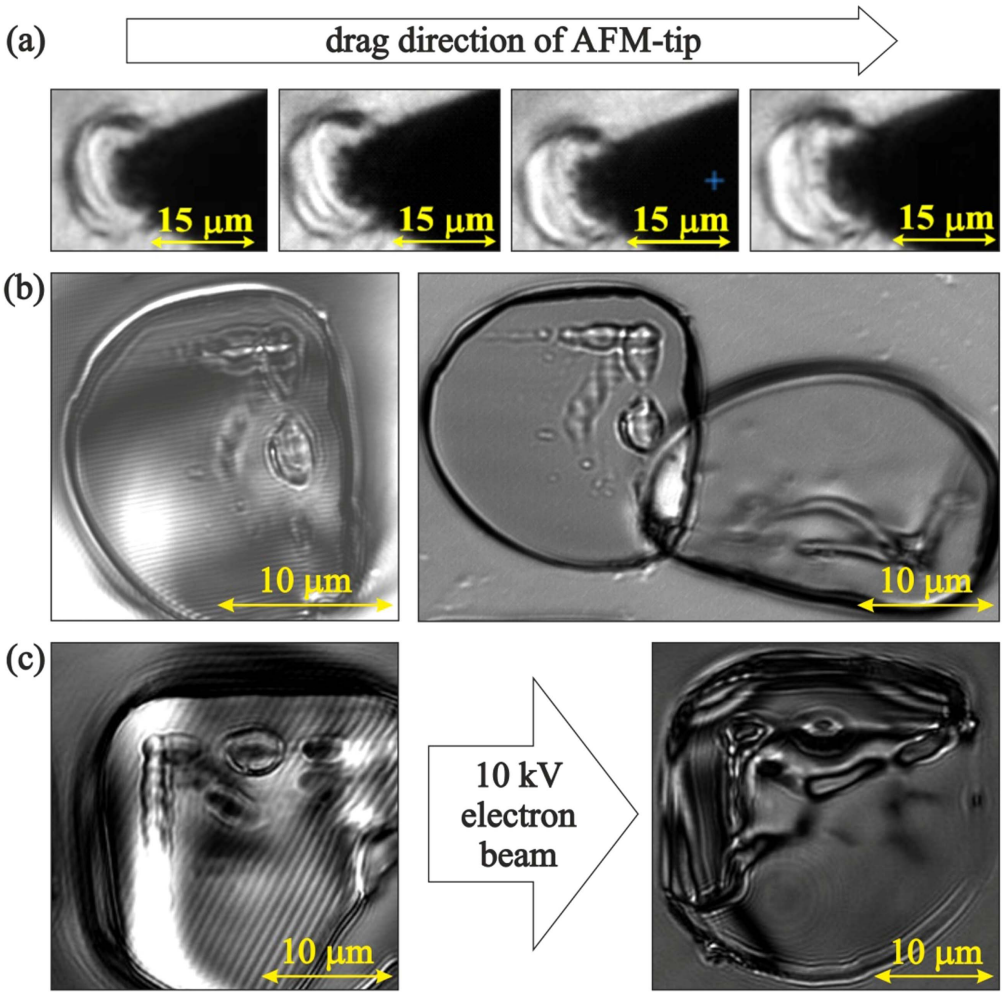

Figure 4. Deletion of SU8-LIPSS (a) series of pictures visualizing the drag of a SU8-LIPSS patch by an AFM tip sticking to it. (b) LSM scans of SU8-LIPSS before (left) and after dislocation by the AFM tip (right) (c) LSM image of SU8-LIPSS before (left) and after exposure to 10 kV electron beam (right).

discovery of an effect which can be described as the deletion of SU8-LIPSS by mechanical stimulation. In most cases even touching SU8-LIPSS with an AFM-tip is enough to completely erase the periodic nanostructure; figures 4(a) and (b) visualize the effect. LSM scans clearly show that the former LIPSS structure in SU8 vanished due to AFM manipulation. Considering that an AFM subjects the substrate to forces in the order of 0.1–1 nN this result is quite surprising. In order to gain a better understanding of the underlying trigger for deletion, the reaction of SU8-LIPSS on different stimuli was investigated. For instance, bending or breaking of the wafer substrate carrying the nanostructured SU8 thin film was found to securely delete all SU8-LIPSS regardless of their position on the substrate. On the contrary, exposure to UVA irradiation below the damage threshold of SU8 ($\sim$0.1 J cm^{-2}, compare figure 2(b)) has no effect on the SU8-LIPSS. The same applies for heat exposure at temperatures up to 250 °C.

Electron irradiation, however, deletes SU8-LIPSS assuredly (figure 4(c)) thus rendering electron microscopy unsuitable for investigations on SU8-LIPSS. The fact that SU8 is not solely utilized in UVA photolithography but also as a negative resist for e-beam lithography explains this observation [32, 33]. Exposure to electron beams in the energy range of 1–100 keV is known to initiate cross linking of SU8, although, the mechanism of this reaction is not fully understood. Both, the direct activation of epoxy groups as well as the dissociation of the sulfonium salt contribute to a cross linking of SU8 exposed to electron irradiation. The resulting polymer differs from its UVA-crosslinked counterpart in several material properties such as the glass transition temperature and the level of mechanical stress [34, 35]. The latter combined with the observations that SU8-LIPSS is highly susceptible to both, bending of the wafer substrate as well as touching with an AFM tip, led to the conclusion that mechanical stress is the key factor for the deletion of the periodic pattern. The reason for this behavior is thought to be related to the process of SU8-LIPSS generation. SU8 is transformed into LIPSS by a single laser pulse impact of 3 ns pulse duration which is a considerably harsh condition of pattern formation. SU8-LIPSS show distinct surface curvature indicating mechanical tension to reside as a result of the rapidly quenched non-equilibrium formation process (figure 5(a)). The dome-like topography of SU8-LIPSS

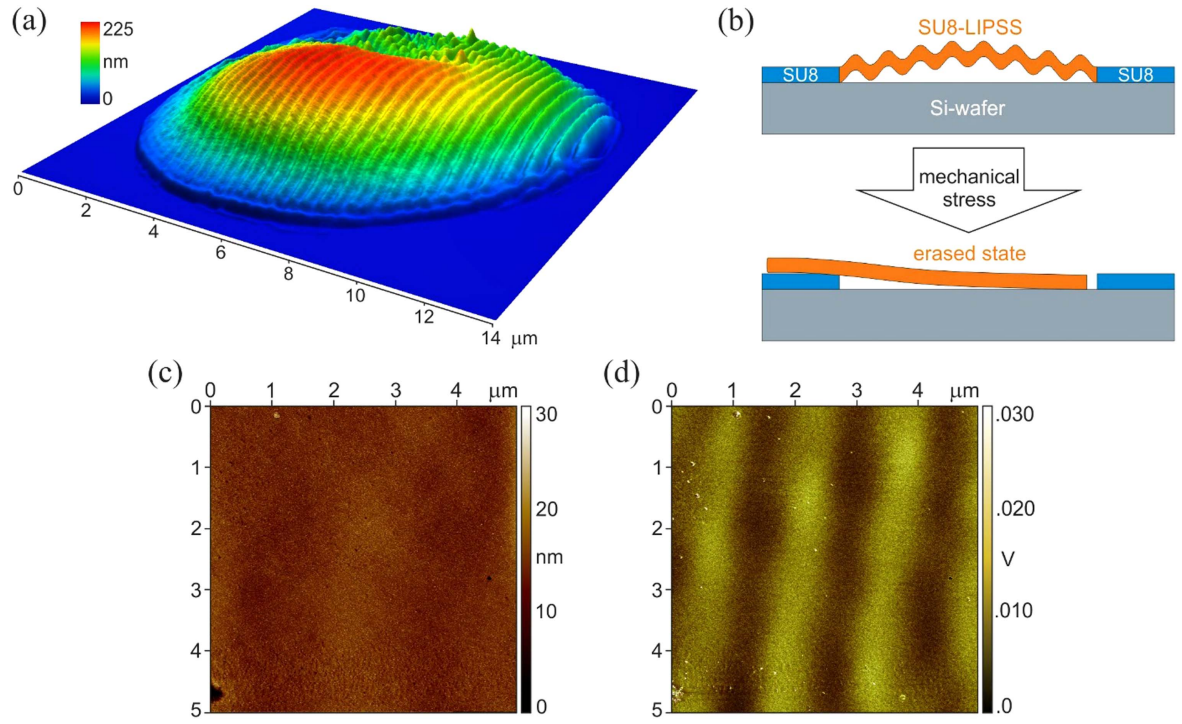

Figure 5. Mechanically stimulated deletion of SU8-LIPSS (a) topographic display of SU8-LIPSS recorded by LSM (b) model of SU8-LIPSS deletion by mechanical stress (c) AFM topography scan of SU8-patch in erased state (d) AFM friction scan of SU8-patch in erased state.

suggests the structure to be wedged in the confinement of the surrounding SU8 thin film. Marginal mechanical stimulation (e.g. by an AFM-tip) is enough to provoke a release from this confinement by slipping the rim of the dome-like structure over the edge of the SU8 thin film (figure 5(b)). Similarly to a pre-loaded spring, the dome unfolds and loses its periodic pattern as soon as the counteracting force providing its stability is abolished. Once switched to the erased state, not only the periodic topography of SU8-LIPSS disappears (figure 5(c)) but also its friction pattern is changed substantially. AFM friction patterns of the erased state (figure 5(d)) show a 20-fold loss in amplitude compared to intact SU8-LIPSS (figure 3(d)). Moreover, the periodicity of the friction pattern changes from 350 to 1400 nm. Attempts to analyze potential structural transformations associated with detected morphological and frictional changes did not succeed due to the lack of appropriate techniques featuring sufficiently high spatial resolution for investigations on SU8-LIPSS.

Conclusion

LIPSS are successfully generated on SU8 thin films by a single laser pulse of 3 ns duration and a laser fluence of 0.18 J cm^{-2}. The periodicity of SU8-LIPSS is 351 nm which is close to the laser wavelength of 355 nm and in good agreement with the surface scattered wave theory. AFM reveals that SU8-LIPSS comprise crosslinked regions that fall together with topographic peaks, and non-crosslinked regions that fall together with topographic valleys in a periodically alternating manner. AFM measurements also demonstrate that SU8-LIPSS is mechanically metastable as the periodic pattern vanishes upon stimulation with forces in the order of nanonewtons. Interestingly, the phenomenon can neither be triggered by temperatures up to 250 °C nor by photonic irradiation below the damage threshold of SU8. The very combination of mechanical metastability with resilience to heat and photonic irradiation makes SU8-LIPSS attractive for applications in the field of passive or rather unpowered systems such as mechanical stress monitors, mechanically erasable memory and micromechanical actuators.

Acknowledgments

Authors and co-authors declare no conflict of interest.

ORCID iDs

Hendrik Reinhardt https://orcid.org/0000-0003-0450-4823

References

[1] Reinitz J 2012 Turing centenary: pattern formation *Nature* **482** 464
[2] Autumn K and Peattie A M 2002 Mechanisms of adhesion in geckos *Integr. Comp. Biol.* **42** 1081–90

[3] Nie Z, Petukhova A and Kumacheva E 2010 Properties and emerging applications of self-assembled structures made from inorganic nanoparticles *Nat. Nanotechnol.* **5** 15–25

[4] Mann S 2009 Self-assembly and transformation of hybrid nano-objects and nanostructures under equilibrium and non-equilibrium conditions *Nat. Mater.* **8** 781–92

[5] Erb R M, Son H S, Samanta B, Rotello V M and Yellen B B 2009 Magnetic assembly of colloidal superstructures with multipole symmetry *Nature* **457** 999–1002

[6] Damasceno P F, Engel M and Glotzer S C 2012 Predictive self-assembly of polyhedra into complex structures *Science* **337** 453–7

[7] Kim H-C, Reinhardt H M, Hillebrecht P and Hampp N A 2012 Photochemical preparation of sub-wavelength heterogeneous laser-induced periodic surface structures *Adv. Mater.* **24** 1994–8

[8] Ito T and Okazaki S 2000 Pushing the limits of lithography *Nature* **406** 1027–31

[9] Kooy N, Mohamed K, Pin L T and Guan O S 2014 A review of roll-to-roll nanoimprint lithography *Nanoscale Res. Lett.* **9** 320

[10] Barbillon G G, Hamouda F and Bartenlian B 2014 Large surface nanostructuring by lithographic techniques for bioplasmonic applications *Manufacturing Nanostructures* (Cheshire: One Central Press)

[11] Öktem B, Pavlov I, Ilday S, Kalaycıoğlu H, Rybak A, Yavaş S, Erdoğan M and Ilday F Ö 2013 Nonlinear laser lithography for indefinitely large-area nanostructuring with femtosecond pulses *Nat. Photon.* **7** 897–901

[12] Reinhardt H, Pietzonka C, Harbrecht B and Hampp N 2014 Laser-directed self-organization and reaction control in complex systems: a facile synthesis route for functional materials *Adv. Mater. Interfaces* **1** 1300060

[13] Tseng M L *et al* 2012 Fast fabrication of a Ag nanostructure substrate using the femtosecond laser for broad-band and tunable plasmonic enhancement *ACS Nano* **6** 5190–7

[14] Birnbaum M 1965 Semiconductor surface damage produced by ruby lasers *J. Appl. Phys.* **36** 3688–9

[15] Emmony D C, Howson R P and Willis L J 1973 Laser mirror damage in germanium at 10.6 μm *Appl. Phys. Lett.* **23** 598–600

[16] Young J F, Preston J S, van Driel H M and Sipe J E 1983 Laser-induced periodic surface structure: II. Experiments on Ge, Si, Al, and brass *Phys. Rev.* B **27** 1155–72

[17] Huang M, Zhao F, Cheng Y, Xu N and Xu Z 2009 Origin of laser-induced near-subwavelength ripples: interference between surface plasmons and incident laser *ACS Nano* **3** 4062–70

[18] Bonse J, Rosenfeld A and Krüger J 2009 On the role of surface plasmon polaritons in the formation of laser-induced periodic surface structures upon irradiation of silicon by femtosecond-laser pulses *J. Appl. Phys.* **106** 104910

[19] Garrelie F, Colombier J P, Pigeon F, Tonchev S, Faure N, Bounhalli M, Reynaud S and Parriaux O 2011 Evidence of surface plasmon resonance in ultrafast laser-induced ripples *Opt. Express* **19** 9035–43

[20] Derrien T J-Y, Krüger J, Itina T E, Höhm S, Rosenfeld A and Bonse J 2013 Rippled area formed by surface plasmon polaritons upon femtosecond laser double-pulse irradiation of silicon *Opt. Express* **21** 29643–55

[21] Sipe J E, Young J F, Preston J S and van Driel H M 1983 Laser-induced periodic surface structure: I. Theory *Phys. Rev.* B **27** 1141–54

[22] Nürnberger P, Reinhardt H, Kim H-C, Yang F, Peppler K, Janek J J and Hampp N 2015 Influence of substrate microcrystallinity on the orientation of laser-induced periodic surface structures *J. Appl. Phys.* **118** 134306

[23] Rodriguez-Rodriguez A, Rebollar E, Soccio M, Ezquerra T A, Rueda D R, Garcia-Ramos J V, Castillejo M and Garcia-Gutierrez M-C 2015 Laser-induced periodic surface structures on conjugated polymers: poly(3-hexylthiophene) *Macromolecules* **48** 4024–31

[24] Barb R A *et al* 2014 Laser-induced periodic surface structures on polymers for formation of gold nanowires and activation of human cells *Appl. Phys.* A **117** 295–300

[25] Rebollar E, Castillejo M and Ezquerra T A 2015 Laser induced periodic surface structures on polymer films: from fundamentals to applications *Eur. Polym. J.* **73** 162–74

[26] Ge C and Cretu E 2017 MEMS transducers low-cost fabrication using SU-8 in a sacrificial layer-free process *J. Micromech. Microeng.* **27** 045002

[27] Li D-L, Wen Z-Y, Shang Z-G and She Y 2016 Thick SU8 microstructures prepared by broadband UV lithography and the applications in MEMS devices *Optoelectron. Lett.* **12** 182–7

[28] Pinto V C, Sousa P J, Cardoso V F and Minas G 2014 Optimized SU-8 processing for low-cost microstructures fabrication without cleanroom facilities *Micromachines* **5** 738–55

[29] He X, Datta A, Nam W, Traverso L M and Xu X 2016 Sub-diffraction limited writing based on laser induced periodic surface structures (LIPSS) *Sci. Rep.* **6** 35035

[30] Shugaev M V, Gnilitskyi I, Bulgakova N M and Zhigilei L V 2017 Mechanism of single-pulse ablative generation of laser-induced periodic surface structures *Phys. Rev.* B **96** 205429

[31] Bolle M and Lazare S 1993 Characterization of submicrometer periodic structures produced on polymer surfaces with low-fluence ultraviolet laser radiation *J. Appl. Phys.* **73** 3516–24

[32] Billenberg B, Jacobsen S, Schmidt M S, Skjolding L H D, Shi P, Boggild P, Tegenfeldt J O and Kristensen A 2006 High resolution 100 kV electron beam lithography in SU-8 *Microelectr. Eng.* **83** 1609–12

[33] Koller D M, Hohenau A, Ditlbacher H, Galler N, Baudrion A-L, Reil F, Schausberger S, Aussenegg F R, Leitner A and Krenn J R 2008 Three-dimensional SU-8 sub-micrometer structuring by electron beam lithography *Microelectr. Eng.* **85** 1639–41

[34] Buijsen P F A 1996 Electron beam induced cationic polymerization with onium salts *PhD Thesis* Delft University of Technology

[35] Rath S K, Boey F Y C and Abadie M J M 2004 Cationic electron-beam curing of a high-functionality epoxy: effect of post-curing on glass transition and conversion *Polym. Int.* **53** 857–62